

Electrical properties of $(\text{Na}_{0.5}\text{Bi}_{0.5})(\text{Zr}_{0.75}\text{Ti}_{0.25})\text{O}_3$ ceramic

Lily¹, K.L. Yadav² and K. Prasad^{*1}

¹University Department of Physics, T. M. Bhagalpur University, Bhagalpur - 812 007, India

²Department of Physics, Indian Institute of Technology, Roorkee - 247 667, India

(Received June 15, 2012, Revised October 30, 2012, Accepted November 14, 2012)

Abstract. Lead-free compound $(\text{Na}_{0.5}\text{Bi}_{0.5})(\text{Zr}_{0.75}\text{Ti}_{0.25})\text{O}_3$ was prepared using conventional ceramic technique at 1070°C/4h in air atmosphere. X-ray diffraction analysis showed the formation of single-phase orthorhombic structure. Permittivity data showed low temperature coefficient of capacitance ($T_{CC} \approx 5\%$) up to 100°C. Complex impedance studies indicated the presence of grain boundary effect, non-Debye type dielectric relaxation and evidences of a negative temperature coefficient of resistance. The ac conductivity data were used to evaluate the density of states at Fermi level and apparent activation energy of the compound.

Keywords: ceramics; electronic materials; dielectric properties; electrical properties; impedance spectroscopy; electrical conductivity

1. Introduction

Complex perovskite with ABO_3 -type structure have received immense attention for the past several years due to their promising applications in various electronic devices e.g. multilayer capacitors, piezoelectric transducers, pyroelectric detectors, electrostrictive actuators, precision micropositioners, etc. Materials used for these applications are mostly lead-based compounds such as: lead zirconate titanate, lead magnesium niobate, lead titanate, etc. Recently, the legislation on waste electrical/electronic equipment (WEEE) and restriction of hazardous substances (RoHS) has been issued by the European Union according to which the use of hazardous substances, such as lead, in electrical parts, is prohibited from 2006 onwards. To meet such requirement, the search for eco-friendly lead-free materials, for these applications has become the field of increasing interest.

Sodium bismuth titanate, $(\text{Na}_{0.5}\text{Bi}_{0.5})\text{TiO}_3$ (abbreviated as NBT) is considered to be an excellent lead-free piezoelectric ceramic material showing strong ferroelectric properties (Rödel *et al.* 2009, Hiruma *et al.* 2009). NBT belongs to perovskite family (ABO_3 -type) with rhombohedral symmetry at ambient temperature and having a Curie temperature, $T_m \sim 320^\circ\text{C}$ (Smolenskii *et al.* 1961, Kreisel and Glazer 2001, Prasad *et al.* 2007). Besides, NBT exhibits an anomaly in its dielectric properties as a result of low temperature phase transition from the ferroelectric to the anti-ferroelectric phase at $\sim 200^\circ\text{C}$ which is termed as depolarization temperature T_d . This T_d is considered to be an important factor for NBT and/or NBT-based ceramics because the

*Corresponding author, Ph.D., E-mail: k.prasad65@gmail.com

piezoelectric response disappears above T_d , which limits their uses for practical applications. During the past few years, several investigations have been made to study the electrical and/or electromechanical properties of the solid solutions of $(\text{Na}_{0.5}\text{Bi}_{0.5})\text{TiO}_3$ with different perovskites e.g.: BaTiO_3 (Hosono *et al.* 2001, Suchanicz *et al.* 2003, Gomah-Petry *et al.* 2004a, Xu *et al.* 2005, Ranjan and Dwiwedi 2005, Watanabe *et al.* 2008, Moon *et al.* 2011, Sun *et al.* 2012), SrTiO_3 (Gomah-Petry *et al.* 2004a, 2004b, Park and Hong 1997, Lee *et al.* 2002, Watanabe *et al.* 2008), PbTiO_3 (Saïd *et al.* 2001, 2004), CaTiO_3 (Saradhi *et al.* 2002a, 2002b, Watanabe *et al.* 2008), $(\text{Ba,Sr})\text{TiO}_3$ (Lee *et al.* 2010), $(\text{K}_{0.5}\text{Bi}_{0.5})\text{TiO}_3$ (Saïd *et al.* 2001, Li *et al.* 2005a, Yoo *et al.* 2004, Isupov *et al.* 2011), $(\text{K}_{0.5}\text{Bi}_{0.5})\text{TiO}_3\text{-BaTiO}_3$ (Li *et al.* 2005b, 2005c, Trelcat *et al.* 2012), etc. for their possible applications in electronic devices. It has also been seen that some of these show better piezoelectric properties while the value of T_d is greatly reduced (Zhao *et al.* 2006, Chu *et al.* 2002). All these attempts have been made to modify the *A*-site i.e., divalent pseudo-cation $(\text{Na,Bi})^{2+}$. Further, it has been observed that modification at *B*-site plays an important role in tailoring various properties of perovskite (Jaiban *et al.* 2012, Li *et al.* 2005d, 2005e, Wada *et al.* 2001, Ishii *et al.* 2001). Recent reports suggested that the NBT-based compositions modified with $\text{Ba}(\text{Cu}_{1/2}\text{W}_{1/2})\text{O}_3$ (Chu *et al.* 2002), $\text{Ba}(\text{Zr,Ti})\text{O}_3$ (Peng *et al.* 2002), ZrO_2 (Lily *et al.* 2008), $\text{Ba}(\text{Ti}_{0.8}\text{Zr}_{0.2})\text{TiO}_3\text{-}(\text{Ba}_{0.7}\text{Ca}_{0.3})\text{TiO}_3$ (Liu and Ren 2009), $(\text{K,Na})\text{NbO}_3$ (Damjanovic *et al.* 2010), KTaO_3 (König *et al.* 2011), $(\text{Ba}_{0.85}\text{Ca}_{0.15})(\text{Ti}_{0.90}\text{Zr}_{0.10})\text{O}_3$ (Gou *et al.* 2012), $(\text{Ba}_{0.98}\text{Ca}_{0.02})(\text{Ti}_{0.94}\text{Sn}_{0.06})\text{O}_3$ (Wu *et al.* 2012), $\text{BaTiO}_3\text{-Ba}_{0.77}\text{Ca}_{0.23}\text{TiO}_3$ (Luo *et al.* 2012), possess improved electrical and/or electromechanical properties. Accordingly, in the present work structural, dielectric, and electrical properties of a new compound $(\text{Na}_{0.5}\text{Bi}_{0.5})(\text{Zr}_{0.75}\text{Ti}_{0.25})\text{O}_3$ (abbreviated hereinafter as NBZT) have been studied. Complex impedance spectroscopy method has been used to analyze the results. The correlated barrier hopping model has been applied to the ac conductivity data to ascertain the conduction mechanism of charge transport in the system. Also, the ac conductivity data have been used to estimate the apparent activation energy and density of states at Fermi level.

2. Experimental details

Polycrystalline $(\text{Na}_{0.5}\text{Bi}_{0.5})(\text{Zr}_{0.75}\text{Ti}_{0.25})\text{O}_3$ was prepared from AR grade (99.9%+ pure) chemicals (Na_2CO_3 , Bi_2O_3 , ZrO_2 and TiO_2) using solid-state reaction method according to the thermochemical reaction: $0.25\text{Na}_2\text{CO}_3 + 0.25\text{Bi}_2\text{O}_3 + 0.75\text{ZrO}_2 + 0.25\text{TiO}_2 \xrightarrow{\Delta} (\text{Na}_{0.5}\text{Bi}_{0.5})(\text{Zr}_{0.75}\text{Ti}_{0.25})\text{O}_3$ at 1070°C for 4 h. The formation of desired compound was checked by X-ray diffraction technique. Requisite amount of polyvinyl alcohol was added as a binder. Cylindrical pellet having a geometrical dimension: thickness = 1.24 mm and diameter = 9.97 mm was made by applying uniaxial stress of ~600 MPa. The pellet was subsequently heated up to 1100°C for 3 h. The XRD pattern was taken on calcined powder of NBZT at room temperature using an X-ray diffractometer (Rikagu Miniflex, Japan) with the help of CuK_α radiation ($\lambda = 0.15418$ nm) over a wide range of Bragg angles ($20^\circ \leq 2\theta \leq 80^\circ$) with a scanning speed 2°min^{-1} . The microstructure of the sintered NBZT sample was taken on the fractured surface using a computer controlled scanning electron microscope (JEOL-JSM840A). The electrical measurements were carried out on a symmetrical cell of type $\text{Ag}|\text{NBZT}|\text{Ag}$, where Ag is a conductive paint coated on either side of the pellet. Electrical impedance (Z), phase angle (θ), loss tangent ($\tan\delta$) and capacitance (C) were measured

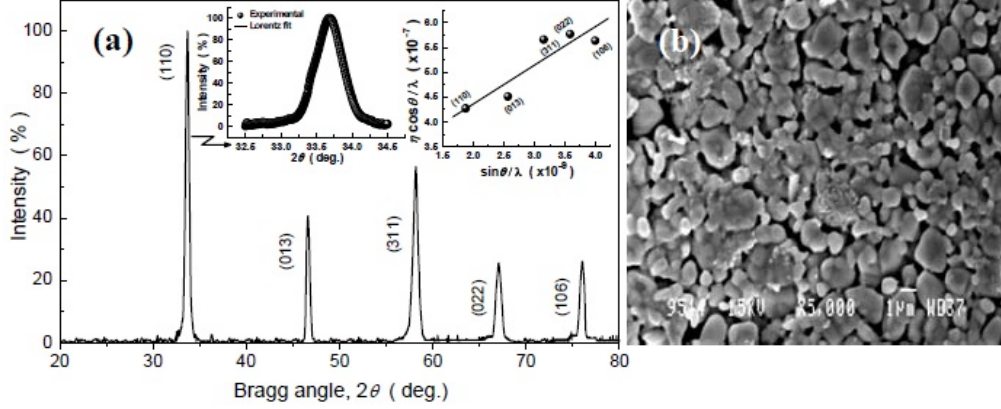


Fig. 1 (a) Indexed X-ray diffraction pattern at room temperature and (b) SEM micrograph with $1 \mu\text{m}$ scale of $(\text{Na}_{0.5}\text{Bi}_{0.5})(\text{Zr}_{0.75}\text{Ti}_{0.25})\text{O}_3$. Inset: Williamson-Hall plot and enlarged view of the XRD (110) peak

as function of frequency (0.1 kHz – 1 MHz) at different temperatures ($40^\circ\text{C} - 500^\circ\text{C}$) using a computer-controlled LCR Hi-Tester (HIOKI 3532-50), Japan. AC conductivity and imaginary part of electric modulus data were thus obtained using the relations: $\sigma_{ac} = t/(AZ')$ and $M'' = \omega C_o Z'$, where Z' is the real part of impedance, t and A are the thickness and area of the sample, respectively.

3. Results and discussion

3.1 Structural and microstructural studies

A standard computer program (POW) was utilized for the XRD-profile (Fig. 1(a)) analysis. Good agreement between the observed and calculated inter-planer spacing (d -values) and no trace of any extra peaks due to constituent oxides, suggested the formation of a single-phase compound having orthorhombic structure. The estimated lattice parameters were: $a = 5.087(6) \text{ \AA}$, $b = 2.996(3) \text{ \AA}$ and $c = 7.694(9) \text{ \AA}$ with an estimated error of $\pm 10^{-4} \text{ \AA}$. The criterion adopted for evaluating the rightness, reliability of the indexing and the structure of NBZT was the minimum value of sum of differences in observed and calculated d -values [i.e., $\sum \Delta d = \sum (d_{obs} - d_{calc})$]. The unit cell volume ($a \times b \times c$) was estimated to be 133.28 \AA^3 . The crystallite size (D) and the lattice strain of NBZT were estimated by analyzing the broadening of X-ray diffraction peaks, using Williamson-Hall approach.

$$\eta \cos \theta = (K\lambda / D) + 2(\Delta\xi / \xi) \sin \theta \quad (1)$$

where η is diffraction peak width at half intensity (FWHM), estimated using Lorentz fit (inset Fig. 1(a)) and $\Delta\xi / \xi$ is the lattice strain and K is the Scherrer constant (0.89). The term $K\lambda/D$ represents the Scherrer particle size distribution. Inset Fig. 1(a) depicts the Williamson-Hall plot for NBZT. A linear least square fitting to $\eta \cos \theta - \sin \theta$ data yielded the values of average crystallite

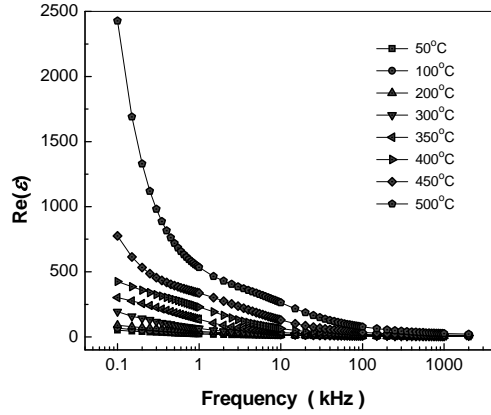


Fig. 2 Variation of real part of dielectric constant of $(\text{Na}_{0.5}\text{Bi}_{0.5})(\text{Zr}_{0.75}\text{Ti}_{0.25})\text{O}_3$ with frequency at different temperatures

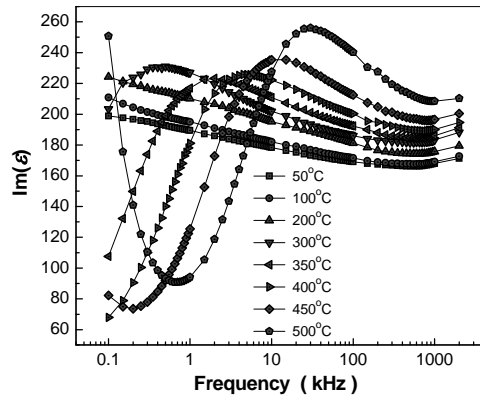


Fig. 3 Variation of imaginary part of dielectric constant of $(\text{Na}_{0.5}\text{Bi}_{0.5})(\text{Zr}_{0.75}\text{Ti}_{0.25})\text{O}_3$ with frequency at different temperatures

size and lattice strain to be 32 nm and 0.0039, respectively. Inset Fig. 1a illustrates the magnified view of the representative (110) peak. A Lorentzian model: $I = I_o + (2A/\pi)[\eta/\{4(\theta - \theta_c)^2 + \eta^2\}]$; where A , η and θ_c are the area, FWHM and centre of the curve, respectively, was applied to analyse the XRD peaks. The fitting parameters as obtained are $I_o = 5.9894$, $A = 75.2311$, $\eta = 0.439$ and $\theta_c = 33.6786$. The value of regression coefficient (r^2) was found to be 0.9889. Fig. 1(b) shows the SEM micrograph of NBZT with 1 μm scale. Grains of unequal sizes ($\sim 0.5\text{-}3 \mu\text{m}$) distributed throughout the sample, are clearly visible in the SEM-micrograph (Fig. 1(b)) of sintered NBZT. The average grain size was estimated to be about 2 μm . The ratio of average crystallite size to the grain size of NBZT is found to be of the order of 10^{-3} .

3.2 Dielectric study

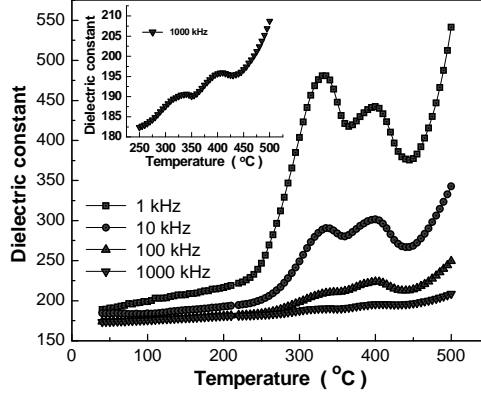


Fig. 4 Temperature dependence of dielectric constant for $(\text{Na}_{0.5}\text{Bi}_{0.5})(\text{Zr}_{0.75}\text{Ti}_{0.25})\text{O}_3$ at different frequencies. Inset shows the enlarged view of the peak area of the plot at 1 MHz

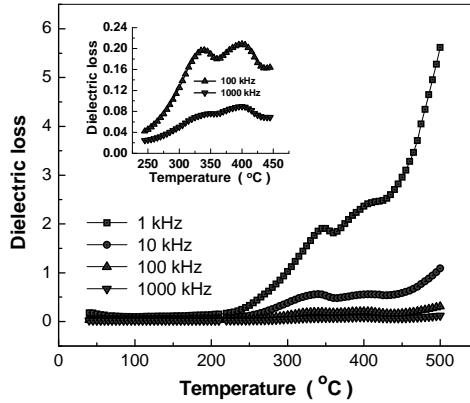


Fig. 5 Temperature dependence of dielectric loss for $(\text{Na}_{0.5}\text{Bi}_{0.5})(\text{Zr}_{0.75}\text{Ti}_{0.25})\text{O}_3$ at different frequencies. Inset shows the enlarged view of the peak area of the plots at 100 kHz and 1 MHz

Figs. 2 and 3 show the frequency dependence of real part (ϵ') and imaginary part (ϵ'') of dielectric constant, respectively at different temperatures. It is observed that ϵ' follows inverse dependence on frequency, normally followed by almost all dielectric/ferroelectric materials. Also, the value of ϵ'' decreases with increase in frequency in the low temperature region, while at higher temperatures, it finds a maximum which shifts to the higher frequency side with the rise of temperature. Dispersion with relatively high dielectric constant can be seen in the ϵ' - f graph in the lower frequency region and the dielectric constant drops at high frequencies. This is due to the fact that dipoles can no longer follow the field at high frequencies. It is evident from Fig. 3 that at low temperatures ϵ'' increases at low frequencies, which indicates the contribution due to electrical conductivity to ϵ^* , and can be expressed as

$$\epsilon^* = \epsilon' - i(\epsilon'' + \sigma / \omega \epsilon_0) \quad (2)$$

Also, with the increase in temperature, relaxation part (referred to as polarization loss) dominates and at higher temperatures (450°C onwards) ε'' consists of two components (following Eq.(2)): the conductivity response of free charges and the frequency dependent polarization loss response of dipoles.

The temperature dependence of dielectric constant (ε') and loss tangent ($\tan\delta$) at different frequencies are shown in Figs. 4 and 5, respectively. The plots show a broad ferro-paraelectric phase transition (i.e., diffuse phase transition, DPT) at 400°C and ε'_m decreases from 442 at 1 kHz to 196 at 1 MHz with the increase in frequency. It is found that both ε' and $\tan\delta$ at room temperature as well as at T_m decrease with increase in frequency. The plots show DPT in neighbourhood of 15°C in NBZT. Also, it is important to note that the addition of Zr^{4+} to NBT shifts T_m as well as T_d (~335°C) to higher temperature side, desirable for piezoelectric applications. Besides, ε - T curves flatten i.e., diffusivity increases with increasing frequency. The broadening in the dielectric peak is a common occurrence in case of solid solutions, which causes deviation from normal Curie-Weiss behaviour, where T_m is not sharp, but physical properties change rather gradually over a temperature range and can be explained by modified Curie-Weiss law

$$1/\varepsilon' - 1/\varepsilon'_m = A(T - T_m)^\gamma \quad (3)$$

where T is temperature, A is a constant and γ (diffusivity parameter) is the critical exponent which can vary from 1, for normal to 1-2 for DPT. A linear regression analysis yielded the value of $\gamma = 1.86$ at 1 kHz, clearly indicating the DPT. The occurrence of DPT in NBZT may be due to the presence of more than one cation in the sub-lattice that should produce some kind of heterogeneities. Further, the temperature coefficient of capacitance (T_{CC}), which is an important parameter for the low-temperature dependence of capacitance, is defined as: $T_{CC}(\%) = [(C_T - C_{RT})/C_{RT}] \times 100$; here C_T and C_{RT} , respectively, represent the values of capacitance at the elevated temperature (100°C) and at the room temperature. It is important to note that the value of ε' is almost temperature insensitive up to 100°C ($T_{CC} \approx 5\%$), which suggests the NBZT to be a potential candidate for capacitor applications. The room temperature values of ε' and $\tan\delta$ at 1 kHz are found to be 189 and 0.18, respectively.

3.3 Complex impedance study

Fig. 6 and its inset show the variation of the real part of impedance (Z') with frequency at different temperatures. It is observed that the magnitude of Z' decreases with the increase in frequency as well as temperature indicates an increase in ac conductivity with the rise in both, temperature and frequency. The Z' values for all temperatures merge above 10 kHz. This may be due to the release of space charges as a result of reduction in the barrier properties of material with the rise in temperature and may be a responsible factor for the enhancement of ac conductivity of material with temperature at higher frequencies (Lily *et al.* 2008). Further, at low frequencies the decrease in Z' values with rise in temperature show negative temperature coefficient of resistance (NTCR) type behaviour like that of semiconductors.

Fig. 7 and its inset show the variation of imaginary part of impedance (Z'') with frequency at different temperatures. It can be seen that the values of Z'' decreases with the increase in frequency up to 300°C and for the temperature $\geq 300^\circ\text{C}$, the Z'' values display a maximum

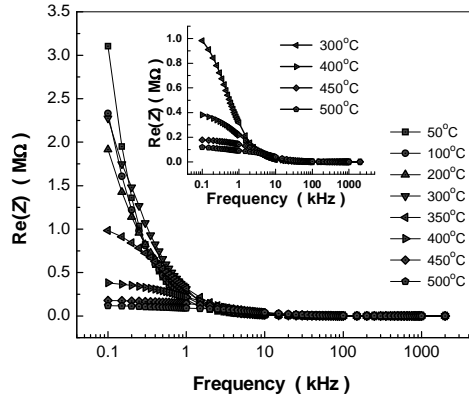


Fig. 6 Variation of real part of impedance of $(\text{Na}_{0.5}\text{Bi}_{0.5})(\text{Zr}_{0.75}\text{Ti}_{0.25})\text{O}_3$ with frequency at different temperatures. Inset shows the representative plots at 300°C, 400°C, 450°C and 500°C

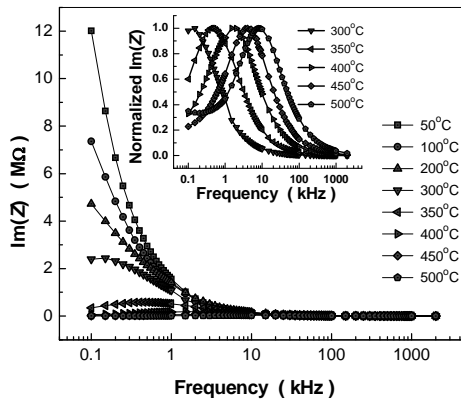


Fig. 7 Variation of imaginary part of impedance of $(\text{Na}_{0.5}\text{Bi}_{0.5})(\text{Zr}_{0.75}\text{Ti}_{0.25})\text{O}_3$ with frequency at different temperatures. Inset shows the scaled imaginary part of impedance with frequency at different temperatures

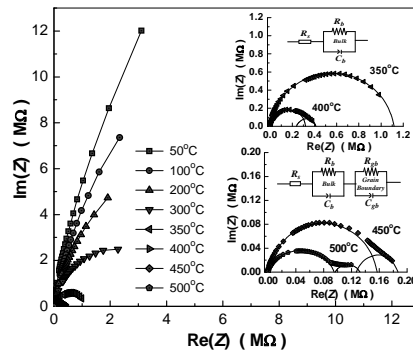


Fig. 8 Complex impedance plot of $(\text{Na}_{0.5}\text{Bi}_{0.5})(\text{Zr}_{0.75}\text{Ti}_{0.25})\text{O}_3$ at different temperatures. Insets: complex impedance plots at some representative temperatures with appropriate equivalent electrical circuits

(Z''_{\max}) which shifts towards higher frequency side with increasing temperature. A typical peak broadening, which is slightly asymmetrical in nature, can be observed with the rise in temperature. The broadening of peaks in explicit plots of Z'' versus frequency suggests a spread of relaxation time *i.e.* the existence of a temperature dependent electrical relaxation phenomenon in the material (Suman *et al.* 2005). The merger of Z'' values in the high frequency region may possibly be an indication of the accumulation of space charge in the material.

Fig. 8 shows the Nyquist diagram for NBZT. It is observed that with the increase in temperature the slope of the lines decreases and the lines bent towards real (Z') axis and at temperature 300°C a semicircle could be traced, indicating the increase in conductivity of the sample. At and above 350°C, two semicircles (inset Fig. 8) could be obtained with different values of resistance for grain and grain boundary. Hence, grain and grain boundary effects could be separated at these temperatures. Also, the maximum of the semicircular plots decrease and the frequency for the maximum shifts to higher values with the increase in temperature. Further, it can be seen that the complex impedance plots (inset Fig. 8) are not represented by a full semicircle, rather the semicircular arc is depressed and the centre of the arc lies below the real (Z') axis, which suggests that the dielectric relaxation in NBZT is of non-Debye type. This may happen due to the presence of distributed elements in the material-electrode system (Macdonald 1987).

Fig. 9 shows the variation of scaled parameters (Z''/Z''_{\max} , M''/M''_{\max} and $\varepsilon''/\varepsilon''_{\max}$) with frequency at 400°C. It can be seen that the peaks are not occurring at the same frequency rather follow the sequence: $f_{Z''} < f_{M''} < f_{\varepsilon''}$. The magnitude of mismatch between the peaks of these parameters represents a change in the apparent polarization. The overlapping of peaks is an evidence of long-range conductivity whereas the difference is an indicative of short-range conductivity (*via* hopping type of mechanism) (Prasad *et al.* 2005).

3.4 AC conductivity studies

In most of the materials, the ac electrical conductivity, due to localized states is given by the Jonscher power law (Jonscher 1977)

$$\sigma_{ac}(\omega) = \sigma(0) + \sigma(\omega) \quad (4)$$

where $\sigma(\omega)$ and $\sigma(0)$ are respectively the frequency dependent and independent part of conductivity. Fig. 10 shows the electrical conductivity versus frequency plots at different temperatures in logarithmic scale. The pattern of the conductivity spectrum shows dispersion throughout the chosen frequency range. The frequency dependence of ac conductivity in such a situation obeys the double power law (Funke 1993)

$$\sigma_{ac}(\omega) = A_1\omega^{s_1} + A_2\omega^{s_2} \quad (5)$$

where A_1 and A_2 are the temperature dependent constants and s_1 and s_2 are temperature as well as frequency dependent parameters. Such dependence is associated with the displacement of carriers which move within the sample by discrete hops of length R between randomly distributed localized sites. The values of the indexes s_1 and s_2 can respectively be obtained from the slopes of the plots $\log \sigma_{ac}$ vs. $\log \omega$ in the low and high frequency regions. Inset Fig. 10 shows the temperature dependence of s_1 and s_2 . It can be seen that the values of both s_1 and s_2 are always less

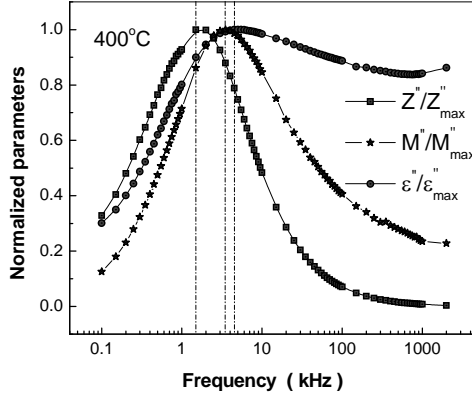


Fig. 9 Variation of normalized Z'' , M'' and ϵ'' with frequency for $(\text{Na}_{0.5}\text{Bi}_{0.5})(\text{Zr}_{0.75}\text{Ti}_{0.25})\text{O}_3$ at 400°C

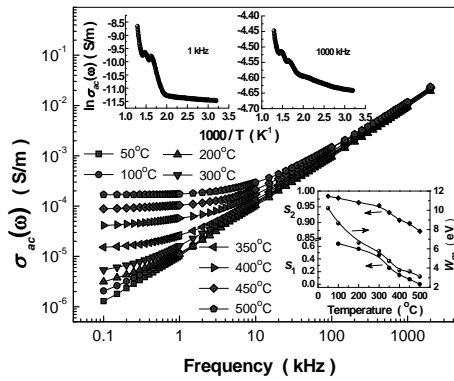


Fig. 10 Variation of ac conductivity with frequency at different temperatures for $(\text{Na}_{0.5}\text{Bi}_{0.5})(\text{Zr}_{0.75}\text{Ti}_{0.25})\text{O}_3$. Inset: Variation of ac conductivity with inverse of temperature at 1 kHz and 1000 kHz. Inset: Variation of s_1 , s_2 and W_m with temperature

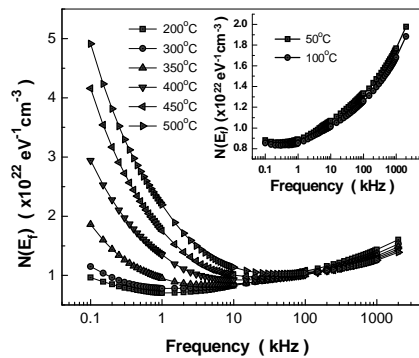


Fig. 11 Variation of $N(E_f)$ of $(\text{Na}_{0.5}\text{Bi}_{0.5})(\text{Zr}_{0.75}\text{Ti}_{0.25})\text{O}_3$ with frequency at different temperatures. Inset shows the variation of $N(E_f)$ with frequency at 50°C and 100°C

than 1 and decrease with the rise of temperature. Further, the value of $s_1 \rightarrow 0$ at higher temperatures indicates that dc conductivity dominates at higher temperatures in the low frequency region and follows Eq. (4). The model based on correlated hopping of electrons over barrier (Elliott 1978) predicts a decrease in the value of the index with the increase in temperature and the theoretical results are thus found to be consistent with the experimental results. Therefore, the electrical conduction in the system could be considered due to the short-range translational type hopping of charge carriers (Funke 1993, Elliott 1978). This indicates that the conduction process is a thermally activated process. Further, the exponent s_i ($i = 1$ or 2) and binding energy (W_m) are related as

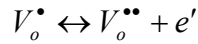
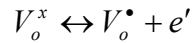
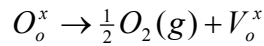
$$s_i = 1 - (6k_B T / W_m) \quad (6)$$

A decreasing trend of W_m with temperature has been observed (inset Fig. 10). The characteristic decrease in slopes (s_1 and s_2) with the rise in temperature is due to the decrease in binding energy.

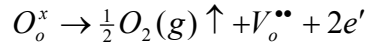
Inset Fig. 10 shows the variation of ac conductivity ($\ln \sigma_{ac}$) versus $10^3/T$ at 1 kHz and 1 MHz. The value of activation energy (E_a) of conduction was obtained using the least squares fitting of the conductivity data in the higher temperature region with the Arrhenius relationship

$$\sigma_{ac} = \sigma_0 \exp(-E_a/k_B T) \quad (7)$$

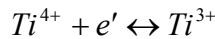
where T is the absolute temperature. The value E_a comes out to be 1.061 eV at 1 kHz and 0.841 eV at 1 MHz. The value of E_a is found to decrease with the increase in frequency. It is considered that ac conductivity is aided by the presence of a small number of free charges, which results in small leakage conduction current, and by displacement of bound charges which give rise to polarization or displacement current in solid dielectrics. Further, ionic conduction plays an important role in ac conductivity at higher temperatures. This may be due to the fact that in the perovskite ferroelectric ceramic samples oxygen vacancies are considered as one of the mobile charge carriers (Kimura *et al.* 1983, Martínez *et al.* 2001). Also, in perovskite titanates, ionization of oxygen vacancy creates conducting electrons, a process which can be described using the Kröger and Vink notation (Kröger and Vink 1956)



Thus excess electrons and oxygen vacancies are formed in the reduction reaction



and these may bond to Ti^{4+} and Zr^{4+} in the form



These electrons are trapped by Ti^{3+} and Zr^{3+} ions or oxygen vacancies to form colour centre (Kimura *et al.* 1983) which can easily be thermally activated into the conduction band.

The ac conductivity data were used to evaluate the density of states at Fermi level $N(E_f)$ using the relation (Sharma *et al.* 2003, Prasad *et al.* 2007)

$$\sigma_{ac}(\omega) = (\pi/3)e^2\omega k_B T \{N(E_f)\}^2 \alpha^{-5} \{\ln(f_o/\omega)\}^4 \quad (8)$$

where e is the electronic charge, f_o the photon frequency and α is the localized wave function, assuming $f_o = 10^{13}$ Hz, $\alpha = 10^{10}$ m⁻¹ at various operating frequencies and temperatures. Fig. 11 shows the frequency dependence of $N(E_f)$ at different temperatures. It can be seen that the value of $N(E_f)$ increases with the increase in operating frequency at room temperature up to 200°C. For temperatures at and above 200°C, the plots show minima which shift towards higher frequency side with the rise in temperature. The reasonably high values of $N(E_f)$ suggests that the hopping between the pairs of sites dominate the mechanism of charge transport in NBZT. Besides, the value of $N(E_f)$ increases with the increment in temperature in the low frequency region while it decreases in the higher frequency region. Therefore, at low frequencies, the electrical conduction in the system is affected by both frequency as well as temperature, whereas at higher frequencies the charge carriers are localized and are affected by thermal excitations.

4. Conclusions

Polycrystalline $(\text{Na}_{0.5}\text{Bi}_{0.5})(\text{Zr}_{0.75}\text{Ti}_{0.25})\text{O}_3$, prepared through a high-temperature solid-state reaction technique, was found to have a single-phase perovskite-type orthorhombic structure. Impedance analyses indicated the presence of grain and grain boundary effects. The value of full width at half maximum is found to be > 1.14 decades. This indicated that the distribution of relaxation times is nearly temperature independent with non-exponential conductivity relaxation behaviour. Sample showed dielectric relaxation which is found to be of non-Debye type and the relaxation frequency shifted to higher side with the increase of temperature. The ac conductivity is found to obey the universal power law. The pair approximation type correlated barrier hopping model is found to successfully explain the universal behaviour of the exponent, s .

References

- Chu, B.J., Chen, D.R., Li, G.R. and Yin, Q.R. (2002), "Electrical properties of $\text{Na}_{1/2}\text{Bi}_{1/2}\text{TiO}_3$ - BaTiO_3 ceramics", *J. Euro. Ceram. Soc.*, **22**(13), 2115-2121.
- Damjanovic, D., Klein, N., Li, J. and Porokhonsky, V. (2010), "What can be expected from lead-free piezoelectric materials?", *Funct. Mater. Lett.*, **3**(1), 5-13.
- Elliott, S.R. (1978), "Temperature-dependence of ac conductivity of chalcogenide glasses", *Philos. Mag.*, **37**(5), 553-560.
- Funke, K. (1993), "Jump relaxation in solid electrolytes", *Prog. Solid State Ch.*, **22**(2), 111-195.
- Gomah-Petry, J.R., Saïd, S., Marchet, P. and Mercurio, J.P. (2004a), "Sodium-bismuth titanate based lead-free ferroelectric materials", *J. Euro. Ceram. Soc.*, **24**(6), 1165-1169.
- Gomah-Petry, J.R., Salak, A.N., Marchet, P., Ferreira, V.M. and Mercurio, J.P. (2004b), "Ferroelectric relaxor behaviour of $\text{Na}_{0.5}\text{Bi}_{0.5}\text{TiO}_3$ - SrTiO_3 ceramics", *Phys. Status. Solidi. B*, **241**(8), 1949-1956.
- Gou, Q., Wu, J., Li, A., Wu, B., Xiao, D. and Zhu, J. (2012), "Enhanced d_{33} value of $\text{Bi}_{0.5}\text{Na}_{0.5}\text{TiO}_3$ - $(\text{Ba}_{0.85}\text{Ca}_{0.15})(\text{Ti}_{0.90}\text{Zr}_{0.10})\text{O}_3$ lead-free ceramics", *J. Alloy. Compd.*, **521**, 4-7.
- Hiruma, Y., Nagata H. and Takenaka, T. (2009), "Thermal depoling process and piezoelectric properties of bismuth sodium titanate ceramics", *J. Appl. Phys.*, **105**(8), 084112-084119.

- Hosono, Y., Harada, K. and Yamashita, Y. (2001), "Crystal growth and electrical properties of lead-free piezoelectric material ($\text{Na}_{1/2}\text{Bi}_{1/2}\text{TiO}_3\text{-BaTiO}_3$)", *Jpn. J. Appl. Phys.*, **40**(9B), 5722-5726.
- Ishii, H., Nagata, H. and Takenaka, T. (2001), "Morphotropic phase boundary and electrical properties of bismuth sodium titanate-potassium niobate solid-solution ceramics", *Jpn. J. Appl. Phys.*, **40**, 5660-5663.
- Jaiban, P., Rachakom, A., Jiansirisomboon S. and Watcharapasorn, A. (2012), "Influences of phase transition and microstructure on dielectric properties of $\text{Bi}_{0.5}\text{Na}_{0.5}\text{Zr}_{1-x}\text{Ti}_x\text{O}_3$ ceramics", *Nanoscale Res. Lett.*, **7**(1), 45-49.
- Jonscher, A.K. (1977), "The 'universal' dielectric response", *Nature*, **267**, 673-679.
- Kimura, T., Machida, M., Yamaguchi, T. and Newnham, R.E. (1983), "Products of reaction between PbO and Nb_2O_5 in molten KCl or NaCl ", *J. Am. Ceram. Soc.*, **66**(10), C195-C197.
- König, J., Spreitzer, M. and Suvorov, D. (2011), "Influence of the synthesis conditions on the dielectric properties in the $\text{Bi}_{0.5}\text{Na}_{0.5}\text{TiO}_3\text{-KTaO}_3$ system", *J. Euro. Ceram. Soc.*, **31**(11), 1987-1995.
- Kreisel, J. and Glazer, A.M. (2001), "High-pressure raman study of a relaxor ferroelectric: The $\text{Na}_{0.5}\text{Bi}_{0.5}\text{TiO}_3$ perovskite", *Phys. Rev. B*, **63**(17), 174106-174116.
- Kröger, F.A. and Vink, H.J. (1956), "Relations between the concentrations of imperfections in crystalline solids", *Solid State Phys.*, **3**, 307-435.
- Lee, J.K., Hong, K.S., Kim, C.K. and Park, S.E. (2002), "Phase transitions and dielectric properties in A-site ion substituted ($\text{Na}_{1/2}\text{Bi}_{1/2}\text{TiO}_3$) ceramics ($A = \text{Pb}$ and Sr)", *J. Appl. Phys.*, **91**(7), 4538-4543.
- Lee, W.C., Huang, C.Y., Tsao, L.K. and Wu, Y.C. (2010), "Crystal structure, dielectric and ferroelectric properties of ($\text{Bi}_{0.5}\text{Na}_{0.5}\text{TiO}_3\text{-(Ba,Sr)TiO}_3$) lead-free piezoelectric ceramics", *J. Alloy. Compd.*, **492**, 307-312.
- Li, Y., Chen, W., Zhou, J., Xu, Q., Sun, H. and Liao, M. (2005a), "Dielectric and ferroelectric properties of lead-free $\text{Na}_{0.5}\text{Bi}_{0.5}\text{TiO}_3\text{-K}_{0.5}\text{Bi}_{0.5}\text{TiO}_3$ ferroelectric ceramics", *Ceram. Int.*, **31**, 139-142.
- Li, Y., Chen, W., Xu, Q., Zhou, J., Gu, X. and Fang, S. (2005b), "Electromechanical and dielectric properties of $\text{Na}_{0.5}\text{Bi}_{0.5}\text{TiO}_3\text{-K}_{0.5}\text{Bi}_{0.5}\text{TiO}_3\text{-BaTiO}_3$ lead-free ceramics", *Mater. Chem. Phys.*, **94**, 328-332.
- Li, Y.M., Chen, W., Xu, Q., Zhou, J. and Gu, X. (2005c), "Piezoelectric and ferroelectric properties of $\text{Na}_{0.5}\text{Bi}_{0.5}\text{TiO}_3\text{-K}_{0.5}\text{Bi}_{0.5}\text{TiO}_3\text{-BaTiO}_3$ piezoelectric ceramics", *Mater. Lett.*, **59**, 1361-1364.
- Li, Y.M., Chen, W., Zhou, J., Xu, Q., Gu, X.Y. and Liao, R.H. (2005d), "Impedance spectroscopy and dielectric properties of $\text{Na}_{0.5}\text{Bi}_{0.5}\text{TiO}_3\text{-NaNbO}_3$ ceramics", *Physica B*, **365**, 76-81.
- Li, Y., Chen, W., Zhou, J., Xu, Q., Sun, H. and Xu, R. (2004e), "Dielectric and piezoelectric properties of lead-free ($\text{Bi}_{0.5}\text{Na}_{0.5}\text{TiO}_3\text{-NaNbO}_3$) ceramics", *Mater. Sci. Eng. B*, **112**, 5-9.
- Lily, Kumari, K., Prasad, K. and Choudhary, R.N.P. (2008), "Impedance spectroscopy of ($\text{Na}_{0.5}\text{Bi}_{0.5}\text{)(Zr}_{0.25}\text{Ti}_{0.75}\text{O}_3$) lead-free ceramic", *J. Alloy. Compd.*, **453**(1-2), 325-331.
- Liu, W. and Ren, X. (2009), "Large piezoelectric effect in Pb-free ceramics", *Phys. Rev. Lett.*, **103**(25), 257602-257605.
- Luo, L., Ni, F., Zhang, H. and Chen, H. (2012), "The enhanced piezoelectric performance of $\text{Bi}_{1/2}\text{Na}_{1/2}\text{TiO}_3\text{-BaTiO}_3$ ceramics by $\text{Ba}_{0.77}\text{Ca}_{0.23}\text{TiO}_3$ substitution", *J. Alloy. Compd.*, **536**, 113-118.
- Macdonald, J.R. (1987), *Impedance spectroscopy: Emphasizing solid materials and systems*, John Wiley and Sons, New York.
- Martínez, O.P., Piñar, F.C. and Barranco, A.P. (2001), "Electrical properties of the ferroelectric bulk in europium-modified lead titanate ceramics", *Solid State Commun.*, **117**(8), 489-493.
- Moon, K.S., Rout, D., Lee, H.Y. and Kang, S.J.L. (2011), "Effect of TiO_2 addition on grain shape and grain coarsening behavior in $95\text{Na}_{1/2}\text{Bi}_{1/2}\text{TiO}_3\text{-5BaTiO}_3$ ", *J. Euro. Ceram. Soc.*, **31**, 1915-1920.
- Park S.E. and Hong, K.S. (1997), "Variations of structure and dielectric properties on substituting a-site cations for Sr^{2+} in ($\text{Na}_{1/2}\text{Bi}_{1/2}\text{TiO}_3$)", *J. Mater. Res.*, **12**(8), 2152-2157.
- Peng, C., Li, J.F. and Gong, W. (2005), "Preparation and properties of ($\text{Bi}_{1/2}\text{Na}_{1/2}\text{TiO}_3\text{-Ba(Ti,Zr)O}_3$) lead-free piezoelectric ceramics", *Mater. Lett.*, **59**(12), 1576-1580.
- Prasad, K., Kumar, A., Choudhary, S.N. and Choudhary, R.N.P. (2005), "Relaxor behaviour in $\text{Pb}[(\text{Mg}_{3/4}\text{Co}_{1/4})_{1/3}\text{Nb}_{2/3}]_2\text{O}_3$ ceramic", *Solid State Ionics*, **176**, 1641-1646.
- Prasad, K., Kumari, K., Lily, Chandra, K.P., Yadav, K.L. and Sen, S. (2007), "Electrical conduction in ($\text{Na}_{0.5}\text{Bi}_{0.5}\text{TiO}_3$) ceramic: Impedance spectroscopy analysis", *Adv. Appl. Ceram.*, **106**(5), 241-246.

- Ranjan, R. and Dwiwedi, A. (2005), "Structure and dielectric properties of $(\text{Na}_{0.5}\text{Bi}_{0.5})_{1-x}\text{Ba}_x\text{TiO}_3$: $0 \leq x \leq 0.10$ ", *Solid State Commun.*, **135**(6), 394-399.
- Rödel, J., Jo, W., Seifert, K.T.P., Anton, E.M., Granzow, T. and Damjanovic, D. (2009), "Perspective on the development of lead-free piezoceramics", *J. Am. Ceram. Soc.*, **92**(6), 1153-1177.
- Saïd, S., Marchet, P., Merle-Méjean, T. and Mercurio, J.P. (2004), "Raman spectroscopy study of the $\text{Na}_{0.5}\text{Bi}_{0.5}\text{TiO}_3$ - PbTiO_3 system", *Mater. Lett.*, **58**(9), 1405-1409.
- Saïd, S. and Mercurio, J.P. (2001), "Relaxor behaviour of low lead and lead free ferroelectric ceramics of the $\text{Na}_{0.5}\text{Bi}_{0.5}\text{TiO}_3$ - PbTiO_3 and $\text{Na}_{0.5}\text{Bi}_{0.5}\text{TiO}_3$ - $\text{K}_{0.5}\text{Bi}_{0.5}\text{TiO}_3$ systems", *J. Euro. Ceram. Soc.*, **21**, 1333-1336.
- Saradhi, B.V.B., Srinivas, K. and Bhimasankaram, T. (2002a), "Impedance and modulus spectroscopy of $(\text{Na}_{1/2}\text{Bi}_{1/2})_{1-x}\text{Ca}_x\text{TiO}_3$ ceramics", *Int. J. Mod. Phys. B*, **16**(31), 4755-4766.
- Saradhi, B.V.B., Srinivas, K. and Bhimasankaram, T. (2002b), "Electrical properties of $(\text{Na}_{1/2}\text{Bi}_{1/2})_{1-x}\text{Ca}_x\text{TiO}_3$ ceramics", *Int. J. Mod. Phys. B*, **16**(27), 4175-4187.
- Sharma, G.D., Roy, M. and Roy, M.S. (2003), "Charge conduction mechanism and photovoltaic properties of 1,2-diazoamino diphenyl ethane (DDE) based schottky device", *Mater. Sci. Engg. B*, **104**(1-2), 15-25.
- Smolenskii, G.A., Isupov, V.A., Agranovskaya, A.I. and Krainik, N.N. (1961), "New ferroelectrics of complex composition", *Sov. Phys. Solid State (Engl. Transl.)*, **2**, 2651-2654.
- Suchanicz, J., Kusz, J., Bhöm, H., Duda, H., Mercurio, J.P. and Konieczny, K. (2003), "Structural and dielectric properties of $(\text{Na}_{0.5}\text{Bi}_{0.5})_{0.70}\text{Ba}_{0.30}\text{TiO}_3$ ceramics", *J. Euro. Ceram. Soc.*, **23**, 1559-1564.
- Suman, C.K., Prasad, K. and Choudhary, R.N.P. (2005), "Impedance spectroscopic studies of ferroelectric $\text{Pb}_2\text{Sb}_3\text{DyTi}_5\text{O}_{18}$ ceramic", *Adv. Appl. Ceram.*, **104**(6), 294-299.
- Sun, Y., Liu, H., Hao, H., Zhang, S., Guo, L. and Yu, Z. (2012), "Effect of $\text{Na}_{0.5}\text{Bi}_{0.5}\text{TiO}_3$ on dielectric properties of BaTiO_3 based ceramics", *Ceram. Int.*, **38S**, S41-S44.
- Trelcat, J.F., Courtois, C., Guiti, M., Leriche, R., Duvigneaud and Segato, P.H.T. (2012), "Morphotropic phase boundary in the BNT-BT-BKT system", *Ceram. Int.*, **38**(4), 2823-2827.
- Wada, T., Toyoiike, K., Imanaka, Y. and Matsuo, Y. (2001), "Dielectric and piezoelectric properties of $(\text{A}_{0.5}\text{Bi}_{0.5})\text{TiO}_3$ - ANbO_3 systems", *Jpn. J. Appl. Phys.*, **40**(9B), 5703-5705.
- Watanabe, Y., Hiruma, Y., Nagata, H. and Takenaka, T. (2008), "Phase transition temperatures and electrical properties of divalent ions (Ca^{2+} , Sr^{2+} and Ba^{2+}) substituted $(\text{Bi}_{1/2}\text{Na}_{1/2})\text{TiO}_3$ ceramics", *Ceram. Int.*, **34**(4), 761-764.
- Wu, B., Xiao, D., Wu, W., Zhu, J., Chen, Q. and Wu, J. (2012), "Microstructure and electrical properties of $(\text{Ba}_{0.98}\text{Ca}_{0.02})(\text{Ti}_{0.94}\text{Sn}_{0.06})\text{O}_3$ -modified $\text{Bi}_{0.51}\text{Na}_{0.50}\text{TiO}_3$ lead-free ceramics", *Ceram. Int.*, **38**(7), 5677-5681.
- Xu, Q., Chen, S., Chen, W., Wu, S., Zhou, J., Sun, H. and Li, Y. (2005), "Synthesis and piezoelectric and ferroelectric properties of $(\text{Na}_{0.5}\text{Bi}_{0.5})_{1-x}\text{Ba}_x\text{TiO}_3$ ceramics", *Mater. Chem. Phys.*, **90**, 111-115.
- Yoo, J., Oh, D., Jeong, Y., Hong, J. and Jung, M. (2004), "Dielectric and piezoelectric characteristics of lead-free $\text{Bi}_{0.5}(\text{Na}_{0.84}\text{K}_{0.16})_{0.5}\text{TiO}_3$ ceramics substituted with Sr", *Mater. Lett.*, **58**, 3831-3835.
- Zhao, S., Li, G., Ding, A., Wang, T. and Yin, Q. (2006), "Ferroelectric and piezoelectric properties of $(\text{Na,K})_{0.5}\text{Bi}_{0.5}\text{TiO}_3$ lead free ceramics", *J. Phys. D Appl. Phys.*, **39**(10), 2277-2281.